PROCEEDINGS, 42nd Workshop on Geothermal Reservoir Engineering
Stanford University, Stanford, California, February 13-15, 2017
SGP-TR-212

The influence of remedial cementing on thermal well design with applications to wellbore integrity

Adonis-Costin Ichim, Catalin Teodoriu and Gioia Falcone

Mewbourne School of Petroleum and Geological Engineering, 100 E Boyd Street, Sarkeys Energy Center, Norman, OK, 73019

adonis.ichim@ou.edu

Keywords: cementing, well design, well integrity

ABSTRACT

The safe operation of geothermal wells is usually achieved with a two-barrier philosophy, similar to that used in oil and gas wells, where production tubing and/or casing constitute the primary barrier to production loads, with the wellbore cement representing the second integrity-assuring element.

Well cement plays an important role in providing well integrity, yet also influences wellbore heat transfer, but its mechanical and thermal properties can vary significantly depending on the mixing method employed, the slurry composition, curing conditions, and human factors. Mechanical strength still represents the major criterion for cement selection, although thermal properties of cements represent an important parameter in the efficient design of geothermal wells.

This paper focuses on the effects of remedial cementing on wellbore integrity and heat transfer, considering how the chosen method of remediation may result in different degrees of efficiency. From experiments designed to reproduce such remedial actions, cement properties are assessed and used to quantify the effect of these procedures on the overall heat transfer in the wellbore, in regards to both thermal stresses and heat exchange. Testing shows that cement mixing with annular fluid during the remedial phase will lead to changes in cement heat transfer properties and may increase the localized wellbore stresses.

1. INTRODUCTION

Wellbore cement is versatile. It provides zonal isolation, casing support and protection, and abnormal pore pressure confinement. The three main techniques of cementing a well are “through the casing”, “inner string”, and “reverse circulation” (Hole, 2008). When cementing through the casing, a pair of plugs (top and bottom) is used with a float collar to displace the volume of cement. Centralizers and scratchers are used on the casing outside and are instrumental for achieving a good casing-to-cement and cement-to-rock bonding. Inner string cementing uses a modified float collar which allows the landing of tubing or drill pipe at the bottom of the well and creates a seal, allowing the pumping of the cement in a shorter time with less losses at the joint (Bourgoyne et al., 1991). In reverse circulation cementing, which is used when weak formations are encountered at the wellbore shoe, the cement slurry is pumped down the annulus and displaces the mud back up the casing. Special tools (e.g. float collar, wellhead) are used in this case. Since the usage of wiper plugs is impossible, the detection of the end of displacement is difficult, making over-displacement by up to 300 ft. a common practice (Bourgoyne et al., 1991).

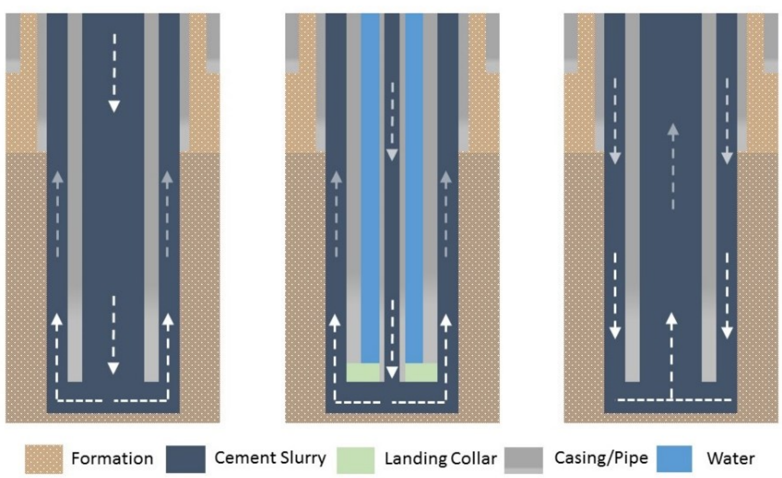

Figure 1 – Main Cementing Techniques

The longevity and integrity of production and injection wells is strongly related to the capacity of the set cement to withstand operational and geological loads, which are directly dependent on the quality of the primary cementing job. Factors influencing the establishment of primary isolation are (Wittmeyer, 2013, King, 2014):

- fracture gradient window
- well inclination
- mud conditioning
- casing centralization, annular clearance
- pipe rotation and/or reciprocation
- pumping flowrate
- pre-flush and cement slurry design (e.g. density, viscosity)
- curing time and temperature

Being able to meet these constraints relates to the geological and operational requirements when designing a well. For example, the depth of a well, together with the fracture gradient window, is crucial when selecting the slurry density, as cement pressure gradients can vary between 0.5 and 1 psi/ft. The pumping flowrate becomes important due to its influence on the equivalent circulating density, which increases the pressure gradient. Overcoming the fracture pressure gradient leads to cement slurry losses and subsequent problems when trying to achieve a certain top of cement depth. Another vital parameter for slurry placement is the bottom-hole circulating temperature, as it reduces the cement setting time. Geothermal wells are usually cased and cemented up to surface in high-temperature environments (>140°C), which tend to be vapor-dominated geothermal, geo-pressured, magmatic or hot dry rock (HDR) systems. These systems are made of hot, hard and abrasive rocks, in naturally fractured and under pressured basins, containing formation fluids that are corrosive with a high solids content (Warner, 2007). These factors pose additional challenges for service companies and operators, who must design the cementing program, according to engineering standards, while taking into account formation challenges and potential operational issues.

Various chemicals and cement formulations are used to address specific problems, which according to the American Petroleum Institute, these can be classified as:

Table 1 – Cement additives and their purpose

Additive	**Purpose and/or Example**
Accelerators	Reduce the ‘waiting on cement’ curing time; salts (calcium or sodium chloride), sea water
Retarders	Enhance the setting time; used in high temperature mediums - sugar; lignosulphonates, hydroxycarboxylic acids, inorganic compounds and cellulose derivatives
Extenders	Lower the density and increase the yield strength; used in weak formations; water, bentonite, sodium silicates, nitrogen, ceramic microspheres
Weighting agents	Increase density; barite, hematite
Dispersants	Polymers used for a better particle distribution
Fluid-loss control agents	Reduce fluid loss; polymers, cellulose
Lost circulation control agents	Mitigate, reduce or prevent circulation loss; various materials
Strength retrogression agents	Used at temperatures higher than 110°C (230°F), where cement’s permeability increases and its strength decreases; silica flour (usually 30 – 40% by weight of cement
Miscellaneous agents	Various applications; anti-foam agents, fibers, latex

Cement blends with 15 to 40% silica flour (API Class A or API Class G) or 30:70 blast furnace slag with API Class A cement are frequently used nowadays. Common additives used for geothermal wells are retarders, friction reducers, fluid loss control agents, free-water control additives, and lost circulation control materials (Hole, 2008). The track record of different cementing operations in high-temperature environments show that even with a properly engineered slurry, suitable cement placement does not occur. Various problems can appear throughout the cementing process, a common one being circulation loss, which diminishes the possibility of getting cement returns to surface and completely cementing the casing string. If circulation loss is observed, a remedial cementing or secondary cementing method must be used, which can be pressurized or non-pressurized. The most common techniques for remedial cementing when cement does not reach the surface are top fill and top squeeze.

Top fill is a method used when good returns reach the surface, but the cement drops back down the annulus while waiting-on-cement to cure. Assuming an air- or liquid-filled annulus, cement is pumped until good returns reach the surface. The top squeeze method is used when no cement returns to surface due to geology, wellbore washouts, or pumping problems. A pre-flush is recommended to remove any fluids which can interfere with the secondary cementing job, after which the squeeze job is performed in a pressurized annulus until pressure remains stable (Rickard, 2012).

An analysis of active Californian geothermal wells' cement jobs shows that the top of cement status is unknown in the majority of the cases (see Figure 1). The available data referred to drilling history and logs of non-commercial and commercial low-temperature wells, observational wells, temperature gradient wells, and water wells.

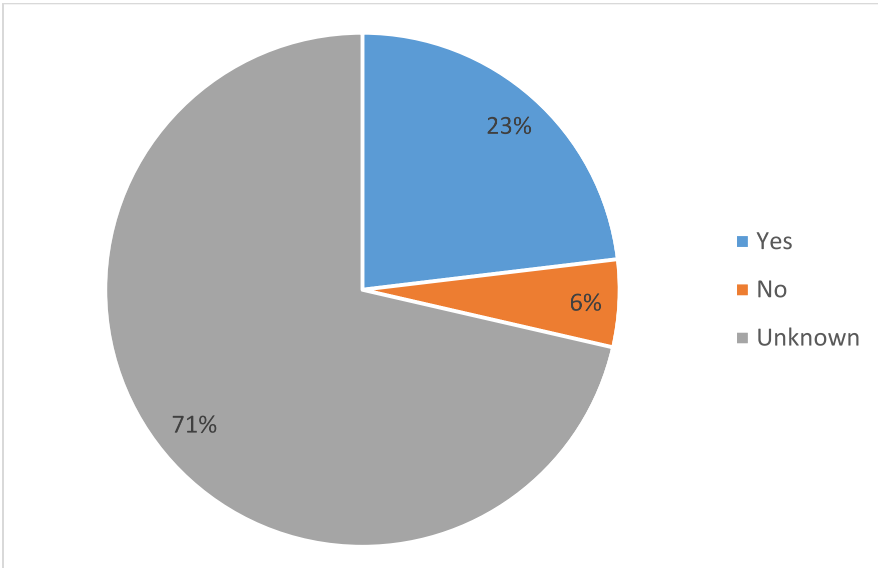

Figure 2 – Top of cement status in Californian geothermal wells (public data)

As outlined in previous work (Ichim et al., 2016 A, 2016 C), the constituency of the cement slurry and the wellbore elements have a direct effect on the wellbore heat transfer. The wellbore overall heat transfer coefficient can be enhanced and diminished by fine-tuning the thermal conductivity of wellbore components as: cement, casing, drilling fluid, etc. Depending on the method, reaction time, the on-site capability to pump additional cement, the slurry properties and the annular fluid on top of the cement, the remedial cement job may have different degrees of efficiency in regards to annular fluid displacement, cement permeability, bonding, strength and set time. This paper focuses on the influence of remedial cementing on cement properties through experiments mimicking secondary cementing procedures.

2. EXPERIMENTAL SETUP FOR THE INVESTIGATION OF REMEDIAL CEMENTING ON TEMPERATURE DISTRIBUTION AND MECHANICAL PROPERTIES

Two pieces of tubing were cemented concentrically in transparent PVC pipes. The following table shows the pipes' geometry, calculated in order to keep the same ratio between pipe outer diameters as in a real well.

Table 2 – Pipes measurements

Item	Length mm	Outer Diameter mm	Inner Diameter mm	Wall Thickness (measured) Mm	Wall Thickness (calculated) mm	Ovality %
Plexiglas	305	114.15	101.42	6.37	6.45	0.261
Tubing	460	33.47	25.89	3.79	3.72	0.471

To replicate top fill procedures, the two pieces of tubing were initially cemented with API Class G cement (1.9 kg/l density) for up to the half of the outer pipe height. The cement was allowed to set for approximately 4 hours, after which a fluid was carefully poured on top of the partially set cement in order to mimic the existence of an annular fluid which would need to be displaced during the remedial cementing job. In Sample 1, the annular fluid was water, whereas in Sample 2, the annular fluid was a low density bentonite drilling fluid (1.02 kg/l). Figure 3 shows the rheological profile of the cement slurry and the drilling fluid, measured with a Fann35 Viscometer.

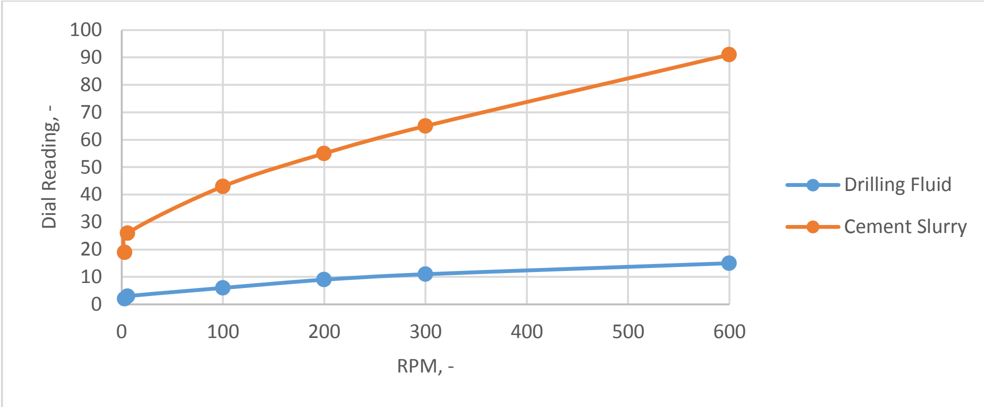

Figure 3 – Rheological profile

A short time after pouring the annular fluid, cement slurry was slowly poured through a glass tube placed on top of the set cement. When cement reached the top of the pipe, the glass tube was removed. This process is shown in the following figures, and the formation of an interface zone between the two cements can be easily noticed.

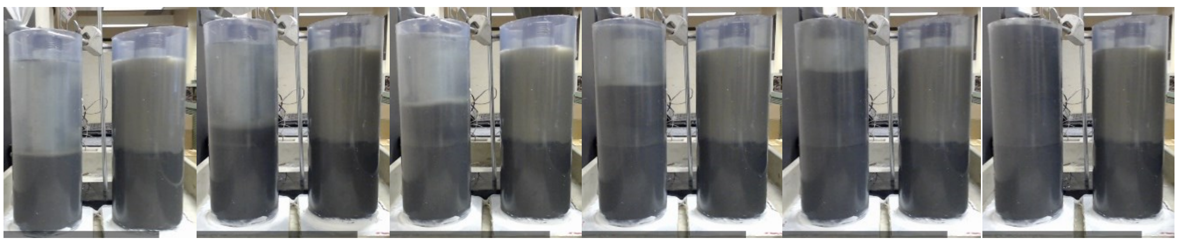

Figure 4 – Displacement of water in the annulus – Left – Sample 1

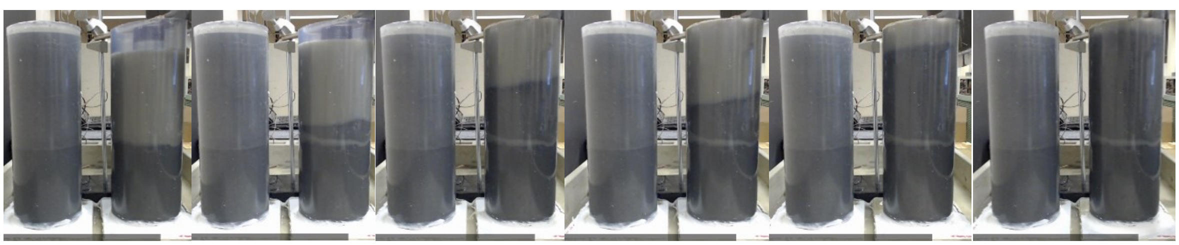

Figure 5 – Displacement of drilling fluid in the annulus – Right – Sample 2

Hydration temperature was monitored through three thermocouples installed in zones of interest (see Figure 7). Temperatures reached 35°C after approximately 5 hours from pouring, and then slowly fell to the ambient temperature of 21 - 23°C over the following 22 hours. Moreover, the same procedure was used when manufacturing cube samples to determine their mechanical properties.

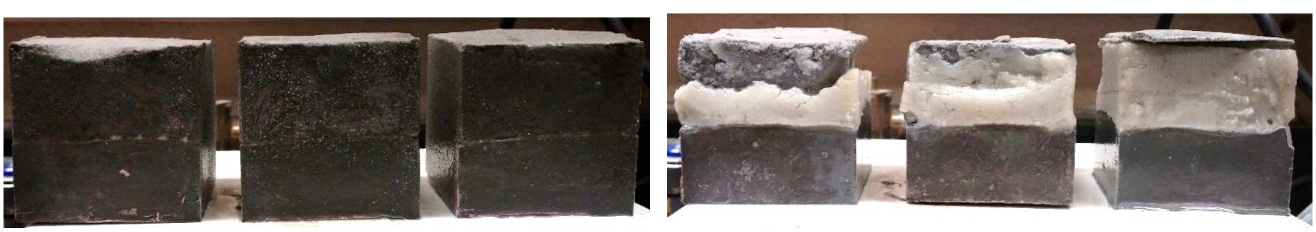

Figure 6 – Cement cubes poured by using top fill comparable procedure; water in annulus (left), mud in annulus (right)

After a period of 40 days, the inside of the tubings is filled with water at 95°C and heating elements are used to keep the temperature constant, until temperature balance is observed at the monitoring points. The 40 days' timeframe is considered sufficient for the cement systems to undergo full hydration and transition from water and anhydrous components to the calcium-silicate-hydrates gel (Thomas et al., 2008). The temperatures inside the tubing and within the cement layer are monitored continuously through thermocouples paired with a DAQ system, as presented in Figure 7. The two samples are heated until temperatures remain constant for approximately 1 hour, after which the heating of the water inside the tubing is stopped, and the cooling of the samples is observed. Additional water at 90°C was added to minimize evaporation effects.

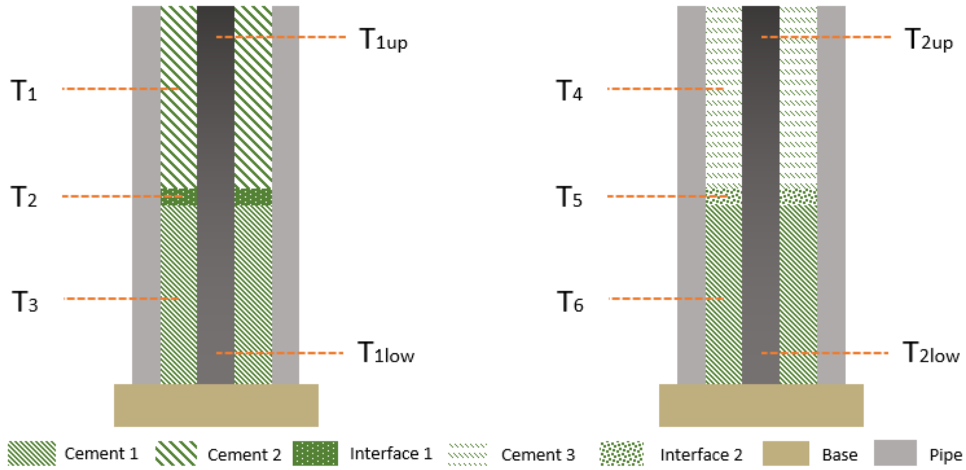

Figure 7 – 2D schematics of thermocouples placement within Sample 1 (left) and Sample 2 (right)

For the cubic samples, the same temperature loading scenario is applied to two out of the three samples for approximately 2 hours in a monitored water bath. One sample is kept at standard conditions to observe pre- and post-heating differences. The Ultrasonic Compressive Strength (UCS) is then acquired via the CM-2500 compression testing machine (ASTM C-39 certified, testing range of 11 – 1,112 kN with an accuracy of ±.5% of indicated load). Prior to measuring the UCS of the samples, the Ultrasonic Pulse Velocity (UPV) is measured with a pair of P-wave transducers (250 kHz). The transducers are placed on the contact zone between the different layers of the cube (cement-cement, cement-drilling fluid mix) with a special coupling fluid, and the force is applied parallel to the contact zone between the layers to simulate the radial expansion of the casing-cement system. The UPV measurements provide a non-destructive testing method which can be used to assess the cement strength development with time under different conditions.

RESULTS AND DISCUSSIONS

Through visual observations, the formation of a gap is observed inside Sample 2 at the contact zone between the two cements during the pouring process. Because of the slow pouring of the cement and its rheological profile, part of the drilling fluid could not be displaced, forming voids both at the interface and within the top cement layer once the drilling fluid gelled. The latter is also caused by the mixing of cement with annular drilling fluid. This behavior is not directly observed in Sample 1, when water is displaced by the cement slurry. However, a minor gap is still present at Interface 1. Nevertheless, even if cement and water mixing occurs, excess water usually separates after a certain time. The temperature measurements for all points of interest (together and separated) are presented in Annex 1. In Figure 8, a comparison between the development of temperatures during the heating phase in the two samples at the interface zone is presented. The values monitored show temperatures inside the contact zones (interfaces) between the two cements. Although the development of the temperatures displays the same trend, higher temperatures (10°C higher or more) are noticed in the case of cement mixed with drilling fluid at Interface 2 in both measurements taken.

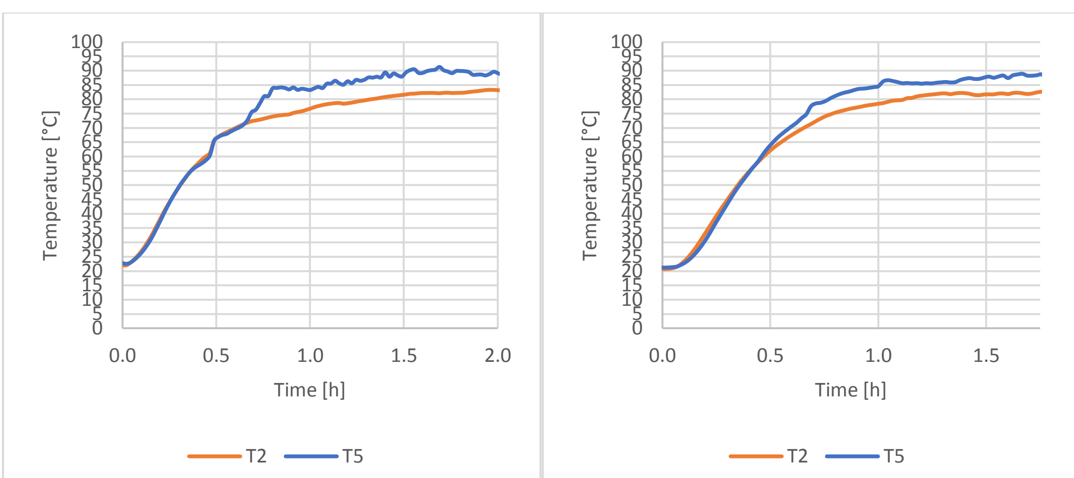

Figure 8 – Heating - Temperature vs. time in the center of the samples – Test 1 (left), Test 2 (right)

This behavior may be explained by the existence of water and drilling fluid rests inside the gap formed at Interface 2, which leads to a much better heat conduction. In a real wellbore, this phenomenon will lead to the development of additional thermal stresses, which may damage the casing-cement-rock system and its integrity through radial and axial expansion.

Based on the measurements and the input geometry of the model's construction, an estimate of the apparent thermal conductivity of the cement at the points of interest can be made. The radial heat flow can be expressed as

$$Q = U_i A_i \Delta T, \quad (1)$$

where Q is expressed in W, the overall heat transfer coefficient (U) in W/m^2-K, the area (A) in m^2 and the temperature difference between the tubing inside and the outermost layer (ΔT) in K. One of the most common forms of the overall heat transfer coefficient is

$$U = \left[\frac{r_{to}}{r_{ti}h_L} + \frac{r_{to}\ln(\frac{r_{to}}{r_{ti}})}{k_{tub}} + \frac{1}{(h_c + h_r)} + \frac{r_{to}\ln(\frac{r_{co}}{r_{ci}})}{k_c} + \frac{r_{to}\cdot\ln(\frac{r_{wb}}{r_{co}})}{k_{cem}}\right]^{-1}, \quad (2)$$

where r represents the radius of the different elements (m), h is the heat transfer coefficient (convection and/or radiation) (W/m^2-K) and k is the thermal conductivity (W/m-K). Applied to this experimental setup, heat transfer by convection and radiation together with conduction through the tubing can be neglected. This leads to the simplified form of

$$U = \left[\frac{r_{to}\cdot\ln(\frac{r_{obs}}{r_{to}})}{k_{cement}}\right]^{-1}, \quad (3)$$

with r_{obs} being the radial distance from the center of the setup to the thermocouple (m) and r_{to} the outer radius of the inner pipe. By replacing equation (3) in equation (1), the following form for the estimation of k_{cement} results:

$$k_{cement} = \frac{Q\ln(\frac{r_{obs}}{r_{to}})}{2\pi\Delta T\Delta L}. \quad (4)$$

The following table presents some estimates of the cement thermal conductivity at a constant heat of 300W, delivered by the heating elements, while assuming a unit incremental length ($\Delta L = 1\,m$). ΔT represents the temperature difference between the inside of the tubing and the observation point after equilibrium is reached inside the tubing. Equilibrium points are defined here as those points in which the temperature difference between the water at the top and the bottom of the tubing is less than 5°C.

Table 3 – Thermal conductivities at the observation points for different temperature differences

Upper Cement 1		**Center Cement 1**		**Lower Cement 1**		**Upper Cement 2**		**Center Cement 2**		**Lower Cement 2**	
$\Delta T, °C$	$k, \frac{W}{m°C}$	$\Delta T, °C$	$k, \frac{W}{m°C}$	$\Delta T, °C$	$k, \frac{W}{m°C}$	$\Delta T, °C$	$k, \frac{W}{m°C}$	$\Delta T, °C$	$k, \frac{W}{m°C}$	$\Delta T, °C$	$k, \frac{W}{m°C}$
21.73	0.65	21.83	0.65	20.76	0.68	21.25	0.66	15.27	0.92	29.24	0.48
21.38	0.66	21.58	0.65	20.40	0.69	20.81	0.68	14.85	0.95	28.47	0.50
20.95	0.67	21.23	0.67	19.92	0.71	20.47	0.69	14.81	0.95	27.8	0.51
20.54	0.69	20.92	0.68	19.50	0.72	20.09	0.70	14.54	0.97	27.1	0.52
20.17	0.70	20.63	0.68	19.15	0.74	19.84	0.71	14.30	0.99	26.56	0.53
19.94	0.71	20.45	0.69	18.81	0.75	19.59	0.72	14.06	1.00	26.02	0.54

In agreement with the temperature measurements, the estimates of thermal conductivity show large values for the interface zones (Center Cement 2) at the center of the Sample 2. Values of the bottom cement (Lower Cement 1 and 2), mixed and poured according to API guidelines, are comparable to experimentally determined values reported by Santoyo et al. (2001), Baghban et al. (2012). The conductivities of the cement in Sample 1 are rather uniform, whereas in Sample 2, conductivities range from 0.48 to 1 W/m-°C.

Measurements were performed on the cubes presented in the previous section after finishing the temperature tests on Sample 1 and 2. The results of the UCS and UPV measurements are presented in Figure 10. All samples were cured for 40 days at atmospheric pressure. Table 3 shows nomenclature and observations regarding the samples.

Table 4 – Cement cubes nomenclature and observation

Name	Temperature	Observation
Standard	20°C	Class G Cement mixed according to API guidelines
Annular Water	20°C	Cement poured by method identical to top fill Cement displaced water from annuls
Annular Water, T	20° to 90°C over two hours	
Annular Mud	20°C	Cement poured by method identical to top fill Cement displaced drilling fluid from annuls
Annular Mud, T	20° to 90°C over two hours	

The following two figures present the results of the crush tests for all the probes. In Figure 9 – Top, representing top cement displacing water, it is obvious that the top fill facilitates the formation of a weak plane in the cubes, and that initiation of a crack and cube failure will take place at that point. In Figure 9 – Bottom, the displacement of drilling fluid through laboratory methods on a small scale was not possible, leading to small or non-existing bond between the two layers of cement.

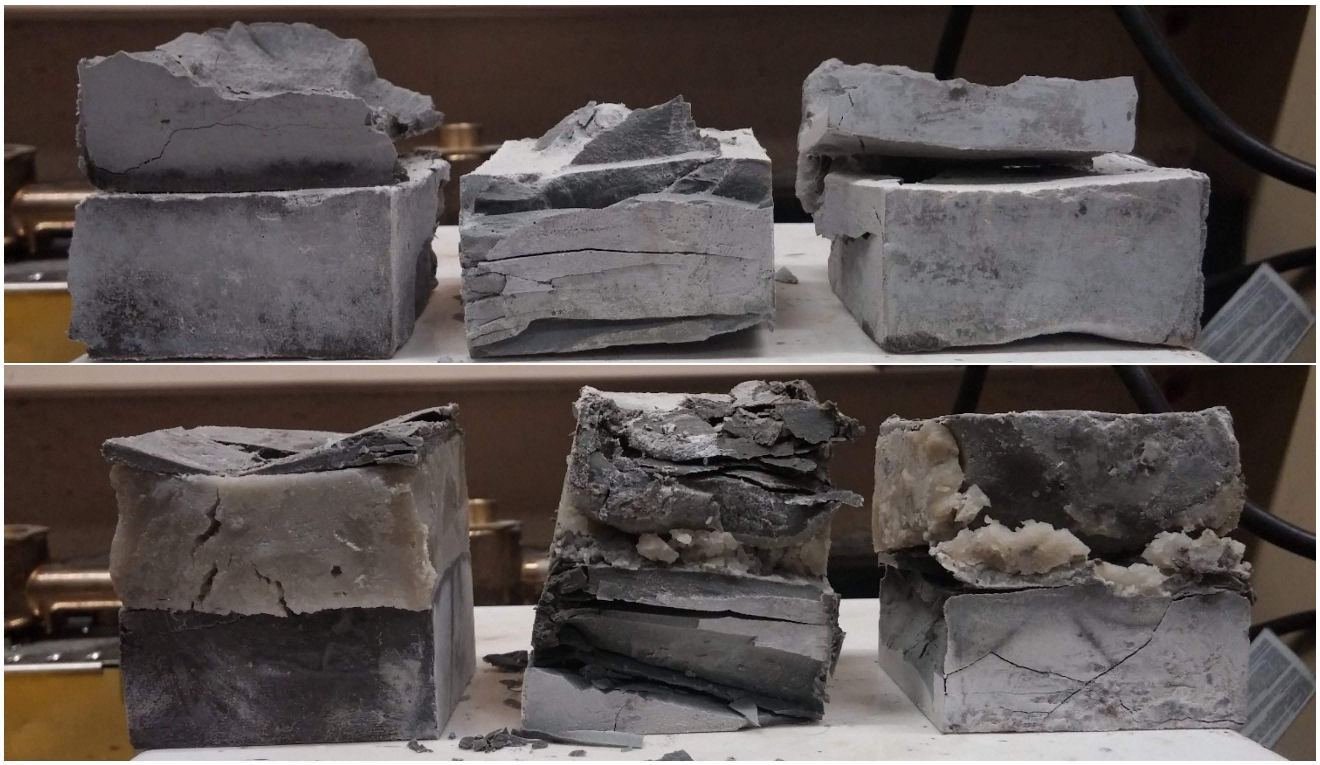

Figure 9 – Cube samples – top poured in annular water, bottom poured in drilling fluid, left samples kept at surface conditions, the other two samples exposed to 20°-90°C over 2 hours

The results of the crush tests and UPV measurements are presented in Figure 10 and show the difference between samples made according to API guidelines, samples poured in water, and samples poured in drilling fluid (mud), as well as the influence of temperature loading on the UCS and UPV.

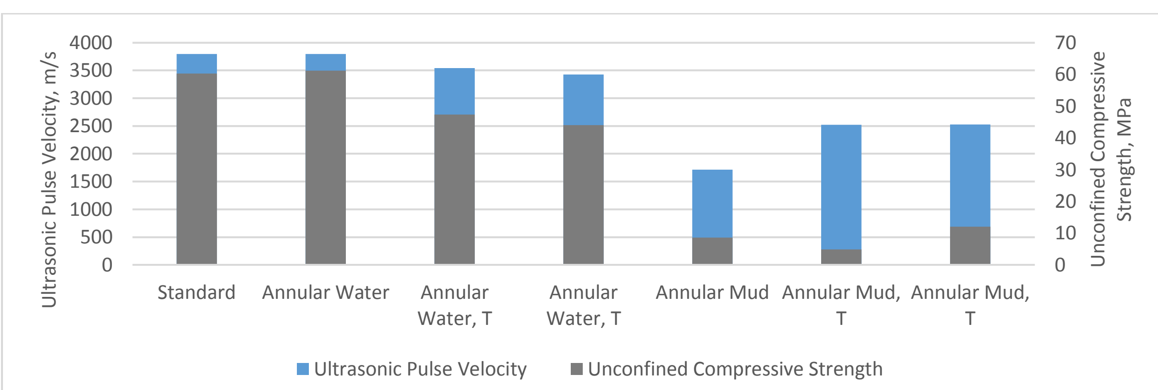

Figure 10 – UPV and UCS tests results

It is observed that the sample poured with water on top resembles the properties of samples prepared per API guidelines and cured for 40 days. However, a clear failure plane at the separation between the two cement pouring stages (similar to the one in Interface 1 – Sample 1) is observed. When casing expansion occurs, this separation plane becomes the weakest point in cement. After exposing these samples to a temperature increase to 90°C for approximately 2 hours, their compressive strength decreases by approximately 30%, but results are comparable. For the samples poured in drilling fluid, the results are rather inconclusive, although, as expected, very low UCS values are achieved of cement mixing with drilling fluid. Also, a change in UPV is noticed for all cases.

CONCLUSIONS

This work attempts to provide a better understanding of the effect of remedial cementing on the temperature distribution in the cement sheath, as well as the mechanical properties of cement poured/pumped during such procedures. Cement properties were assessed and used to quantify the effect of remedial cementing procedures on the overall heat transfer in the wellbore and on the cement mechanical properties.

The development of a gap was observed inside at the contact zone between the two cements during the pouring process. This gap is larger when cement is poured in the drilling fluid. Because part of the drilling fluid could not be displaced, voids formed both at the interface and within the top cement layer once the drilling fluid became thixotropic. The existence of such a gap may threaten well integrity if it extends to surface and/or to another breach in integrity barriers, and weakens the local strength of the casing-cement-rock system.

It was shown that cement mixing with annular fluid during the remedial phase leads to changes in cement heat transfer properties and may increase the localized temperature in the cement sheath and, consequently, the induced thermal stresses. Higher temperatures are observed at the interface between neat cement and cement poured in drilling fluid, when compared to cement poured in water.

Using a simplified heat transfer model, the thermal conductivities of the cement layers were estimated as a function of temperature difference under application of constant heat to the sample. The conductivities of the cement in Sample 1 vary between 0.65 and 0.75 W/m-°C, whereas in Sample 2, conductivities range from 0.48 to 1 W/m-°C.

The assessment of mechanical properties for the samples poured in water shows a 30% decrease in the compressive strength of the samples after an exposure to the temperature loading scenario. A failure plane at the separation between the two cement pouring stages is observed. When casing expansion occurs, this separation plane becomes the weakest point in cement, facilitating cement failure. The local de-bonding will lead again to the above-mentioned localized wellbore temperature increase, which may reduce the ability of the well to withstand operational and geological loads.

As a strong cement bond was not obtained in the cube samples contaminated with drilling fluid, rather inconclusive results were attained. However, very low UCS and high UPV values for the samples poured in drilling fluid are obtained.

REFERENCES

Baghban M. H., Hovde P. J., Jacobsen S. (2012). Analytical and Experimental Study on Thermal Conductivity of Hardened Cement Pastes, Materials and Structures Journal

A.T. Bourgoyne Jr, K.K. Millheim, M.E. Chenevert and F.S. Young Jr. (1991). "Applied Drilling Engineering", SPE Textbook Series Vol. 2, Society of Petroleum Engineering, ISBN: 978-1-55563-001-0

Hole, H. M., (2008). Geothermal Well Cementing, Petroleum Engineering Summer School, Workshop #28, Dubrovnik, Croatia, June 9-13, 2008

Ichim, A. C., Teodoriu, C. (2016, A). Reflections on Overall Heat Transfer Coefficient with Application to Thermal Well Design. Society of Petroleum Engineers. doi:10.2118/182531-MS

Ichim, A. C., Marquez, A., & Teodoriu, C. (2016, B). How Accurate is Your Well Integrity? A Discussion About the Surface Casing Integrity Under Temperature Loading in Heavy Oil Fields. Society of Petroleum Engineers. doi:10.2118/181154-MS

Ichim, A., Teodoriu, C., Falcone, G., (2016, C) Influence of Cement Thermal Properties on Wellbore Heat Exchange, PROCEEDINGS, 41st Workshop on Geothermal Reservoir Engineering, Stanford University, Stanford, California, February 22-24, 2016

King, G.E., (2014, November 18). Basic Cement Isolation Evaluation

Rickard, W.M., Hernández, J., Bailey, A., (2012, November 21 – 23). Top Squeeze or Top Fill: Improved Secondary Cementing for Geothermal Wells, proceedings of the 4th African Rift Geothermal Conference 2012, Nairobi, Kenya

Santoyo E., Garcia A., Morales J.M., Contreras E., Espinosa-Paredes G., (2001). Effective thermal conductivity of Mexican geothermal cementing systems in the temperature range from 28 °C to 200 °C, Applied Thermal Engineering Journal, Elsevier, 2001

Thomas, J., Jennings, H. (2008). Science of Concrete Monograph, Northwestern University, Infrastructure Technology Institute, Evanston, IL, USA

Warner, H.R. Jr., (2007). Petroleum Engineering Handbook, Volume VI: Emerging and Peripheral Technologies, Society of Petroleum Engineers, 2007

Wittmeyer, H. (2013, June 27). Fracking and Well Casing Failure, Frackwire, (http://frackwire.com/well-casing-failure/) (accessed on December 15, 2016)

ANNEX

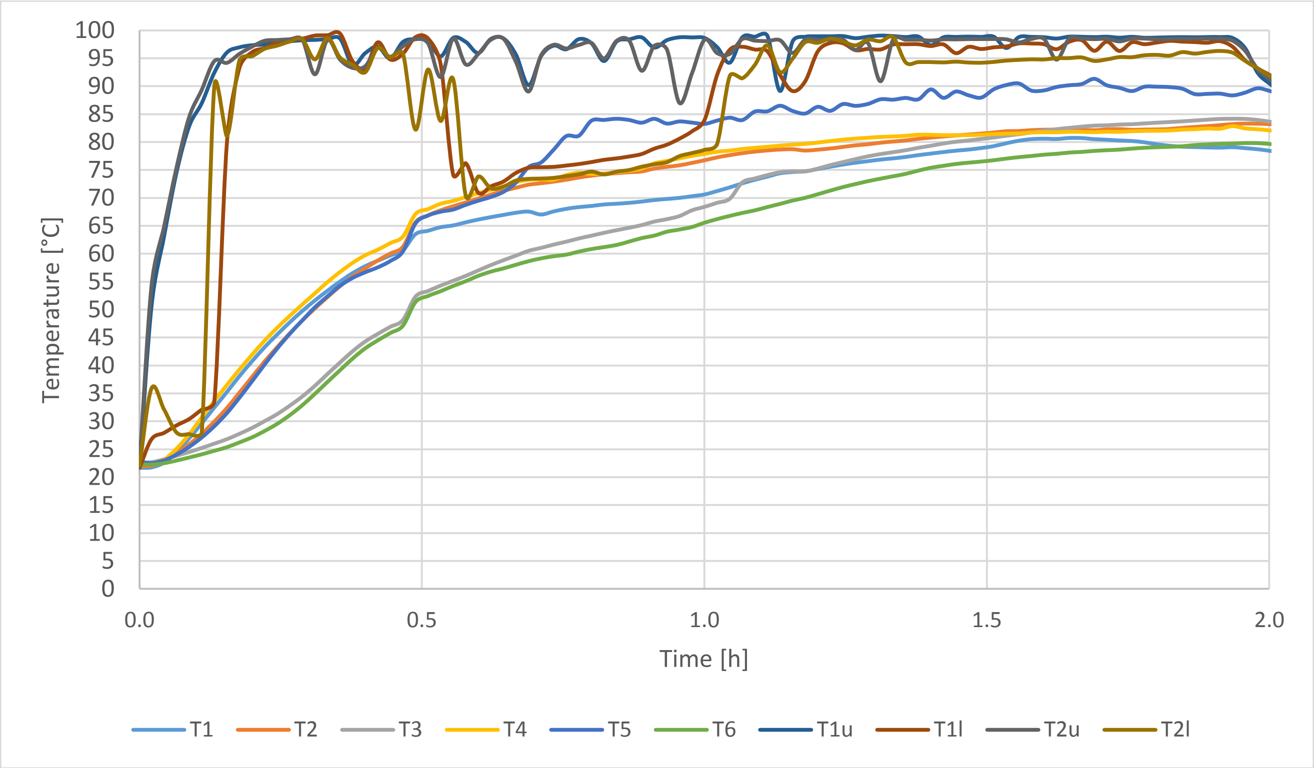

Annex 1 - Test 1 - Temperature monitoring – heating phase

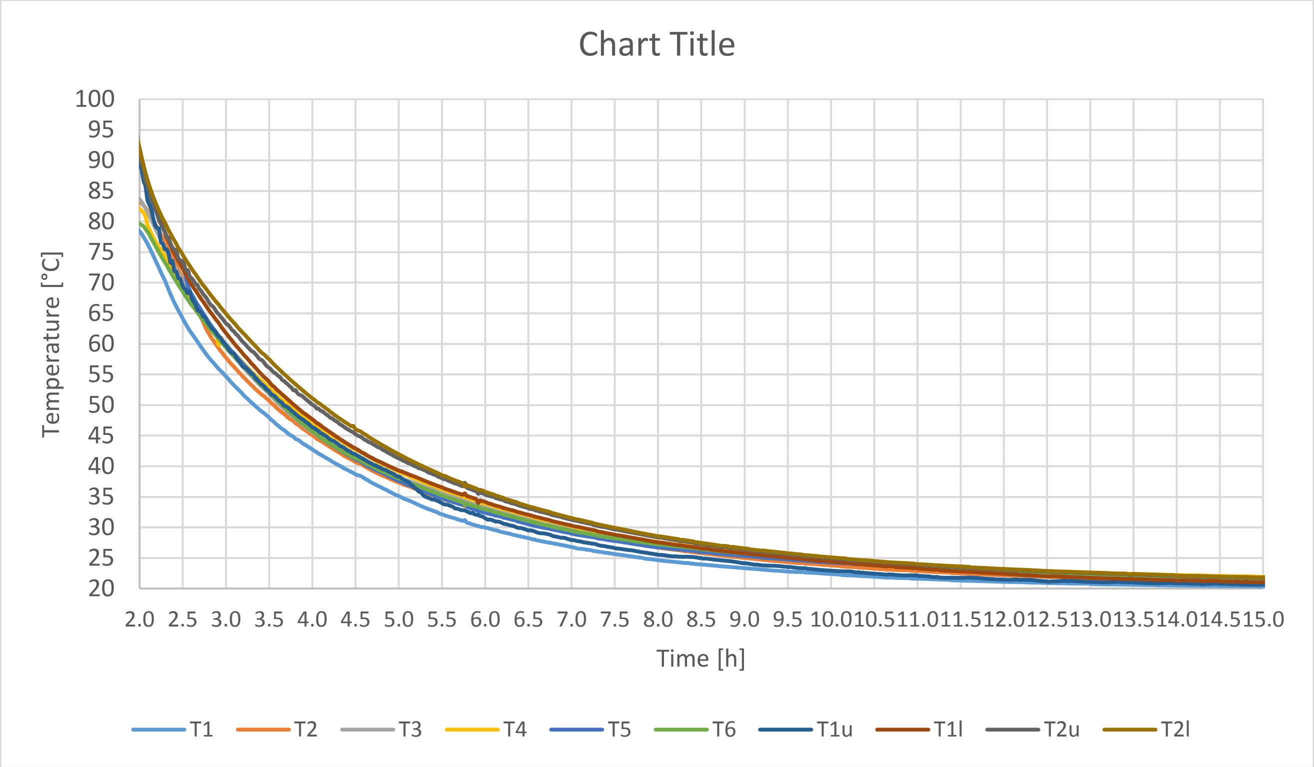

Annex 2 - Test 1 - Temperature monitoring – cooling phase

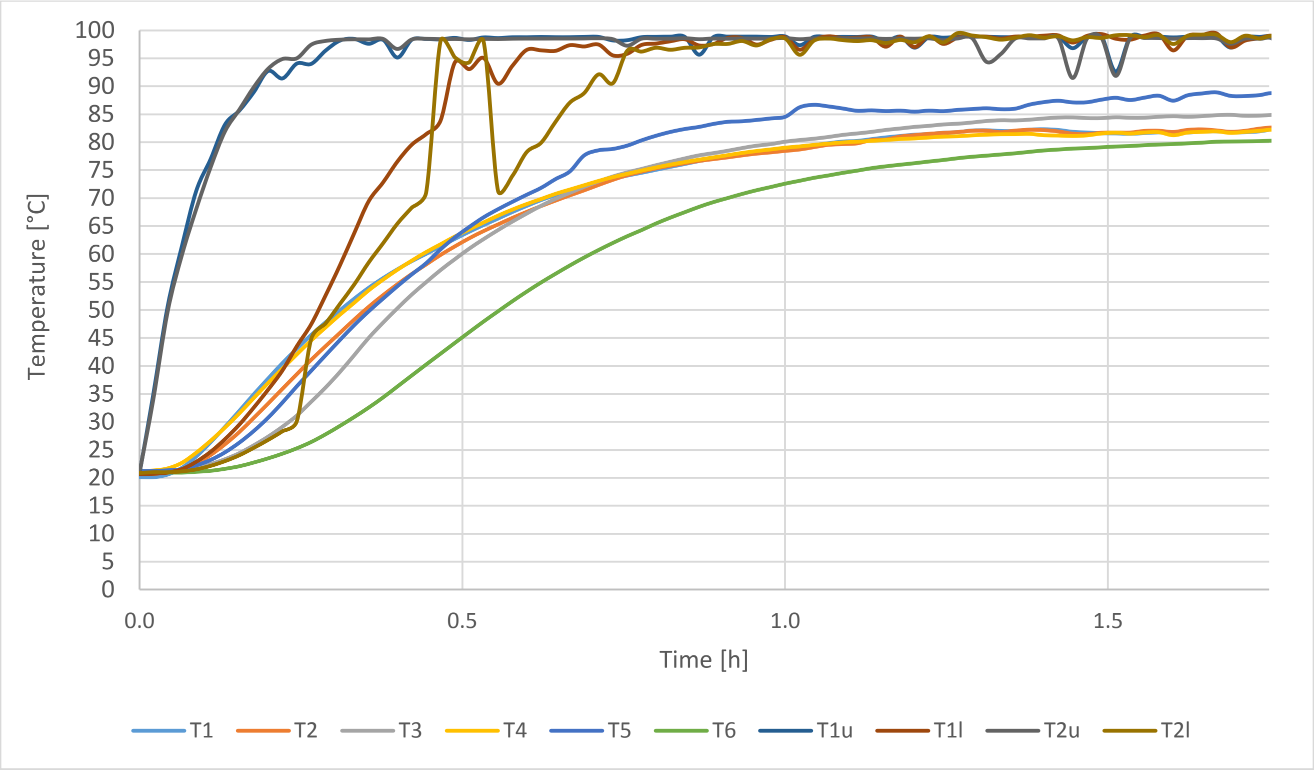

Annex 3 – Test 2 - Temperature monitoring – heating phase

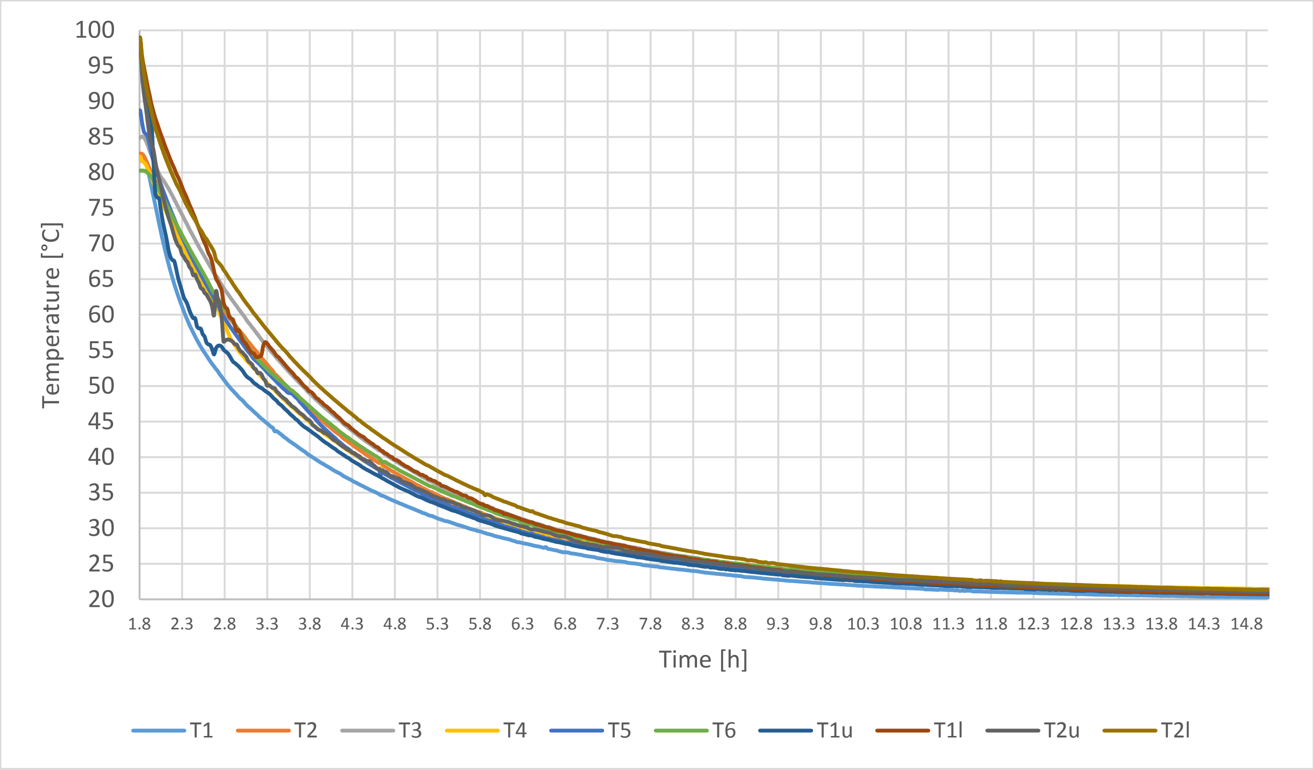

Annex 4 - Test 2 - Temperature monitoring – cooling phase

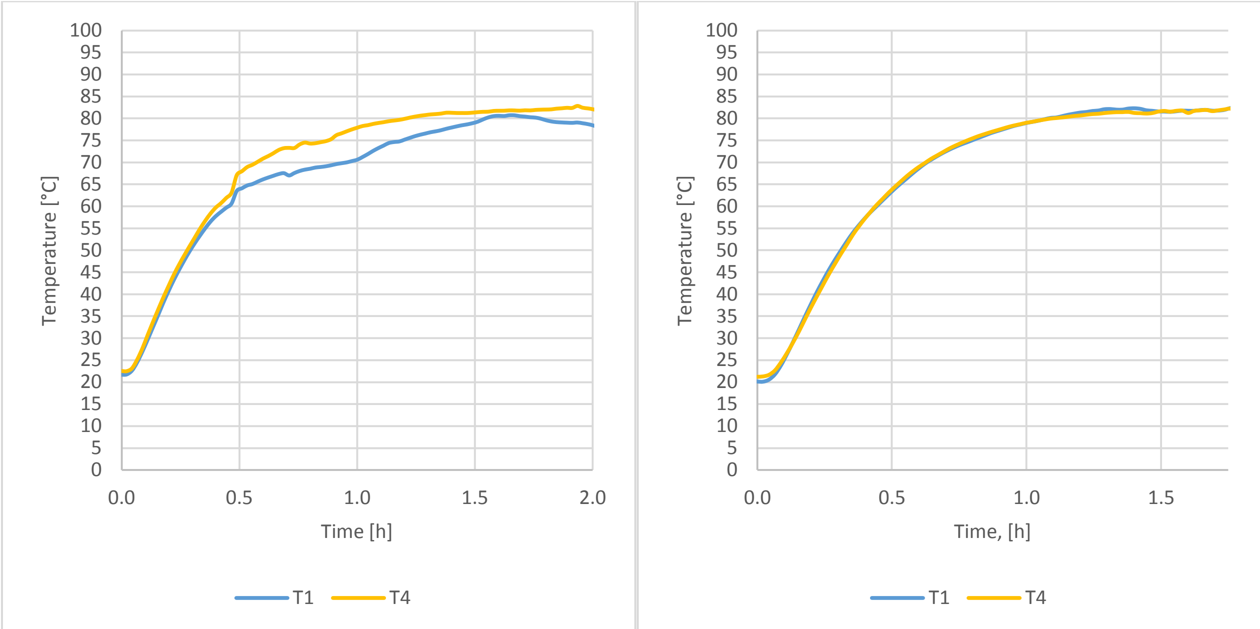

Annex 5 - Heating - Temperature vs. time in the upper part of the samples – Test 1 (left), Test 2 (right)

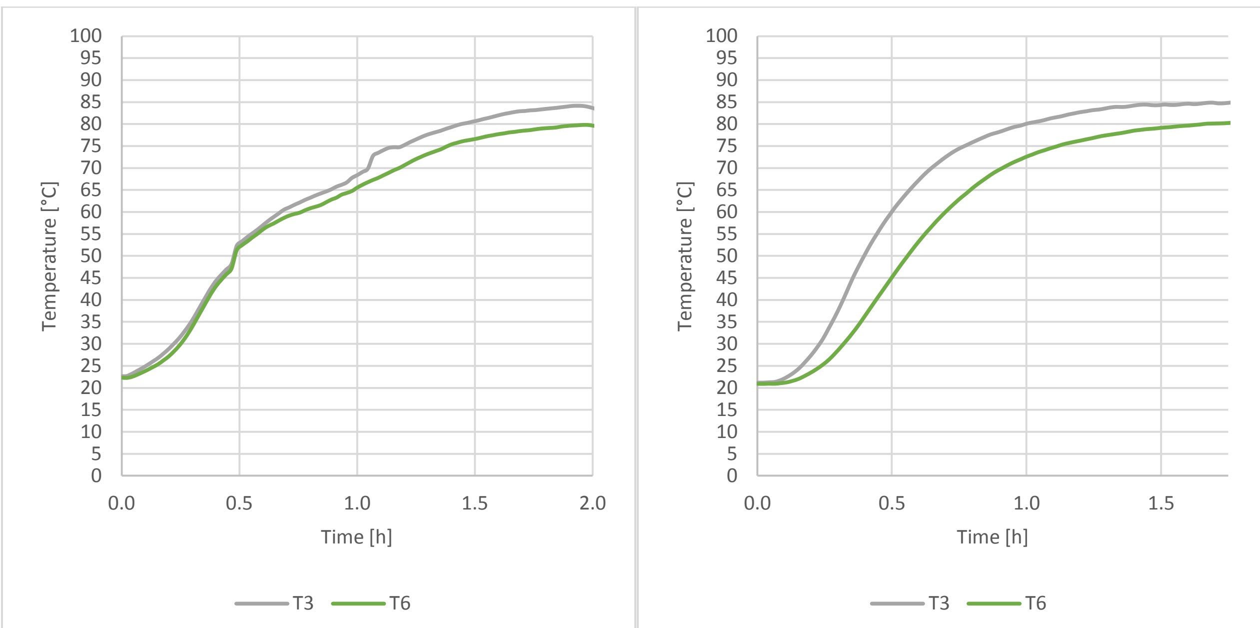

Annex 6 - Heating - Temperature vs. time in the lower part of the samples – Test 1 (left), Test 2 (right)

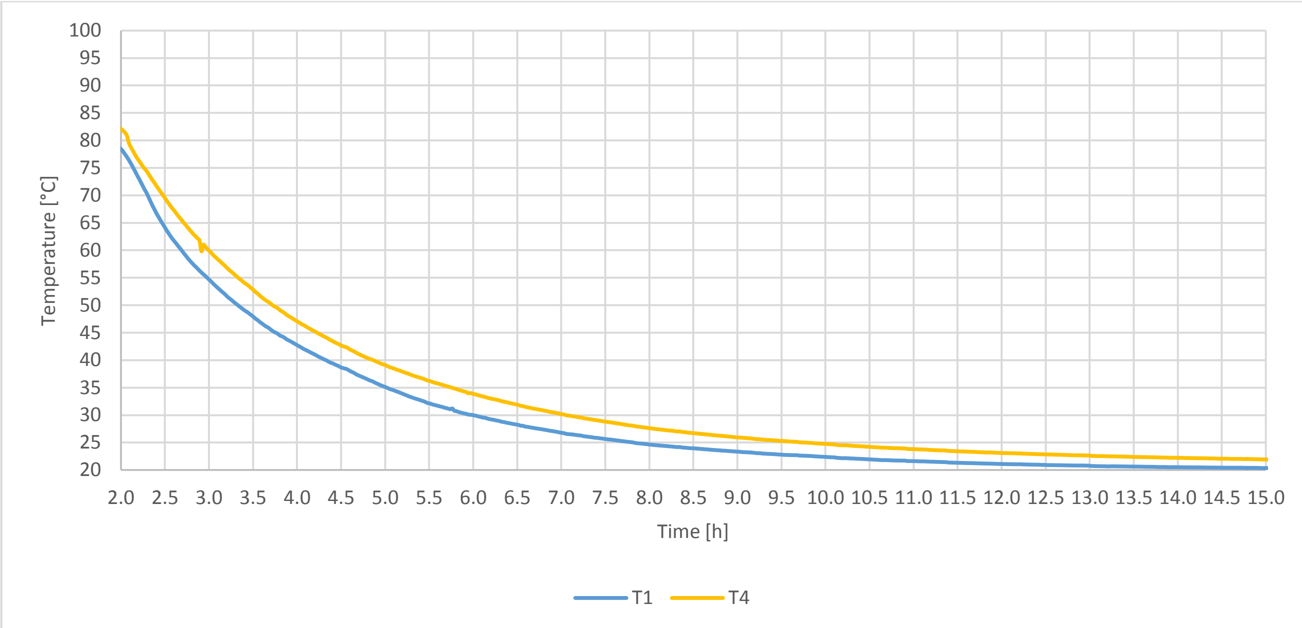

Annex 7 - Cooling - Temperature vs. time in the upper part of the sample – Test 1

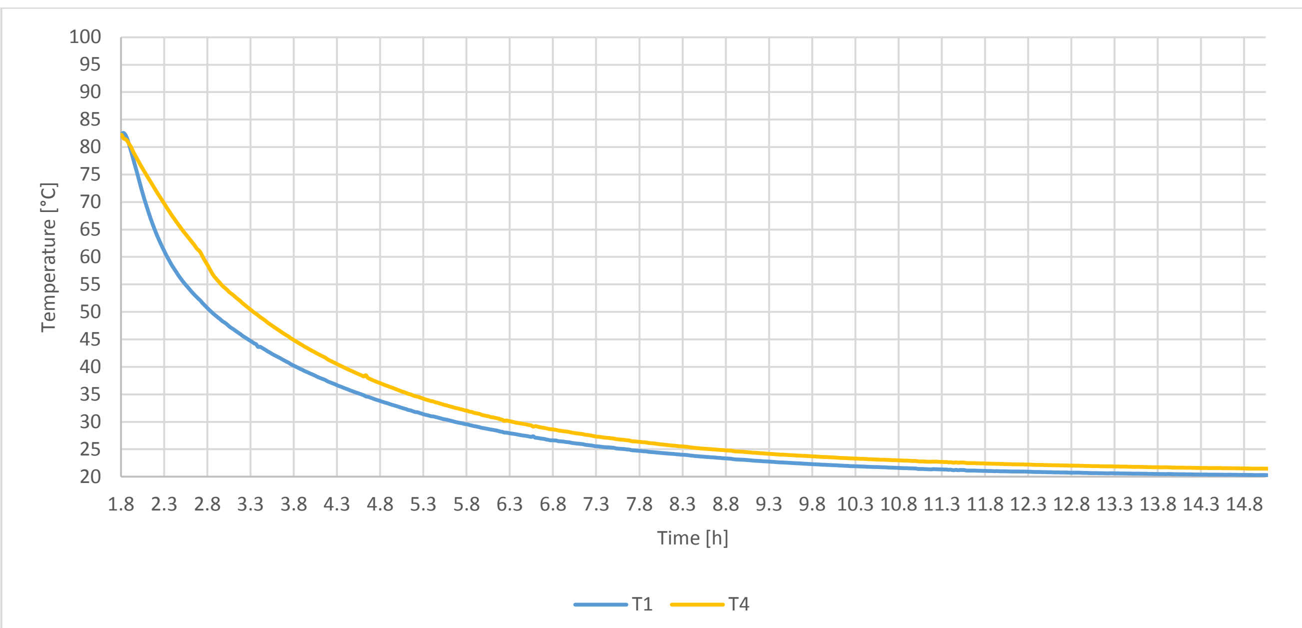

Annex 8 - Cooling – Temperature vs. time in the upper part of the sample – Test 2

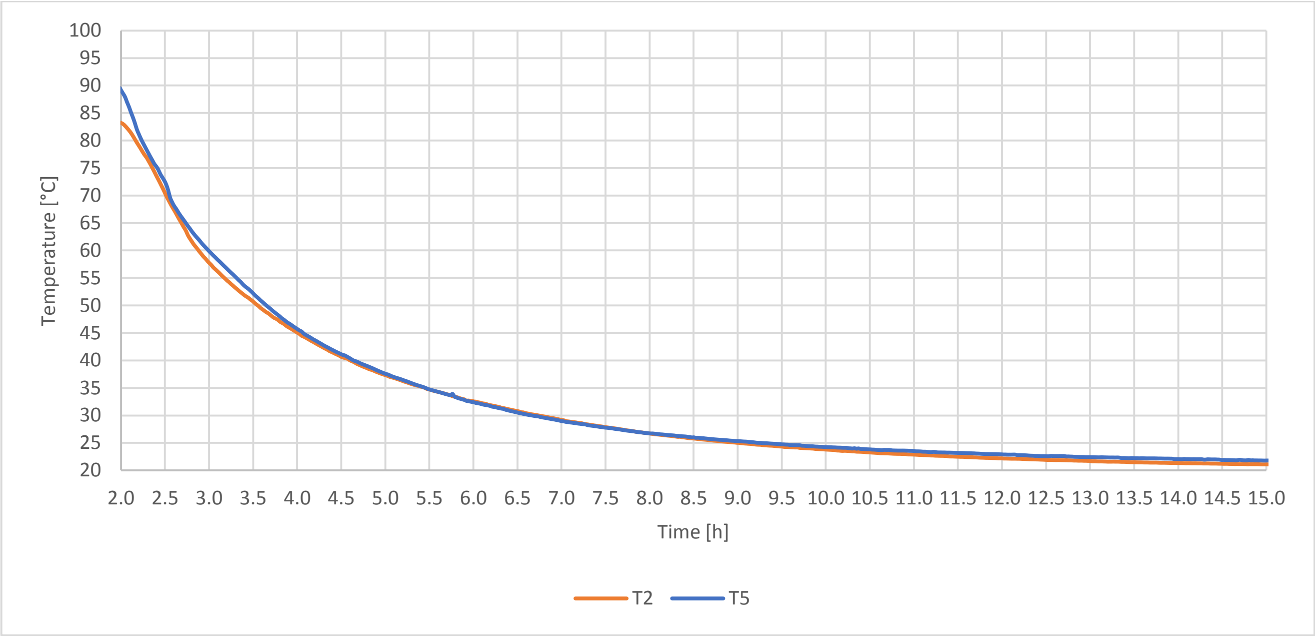

Annex 9 - Cooling – Temperature vs. time in the center of the sample – Test 1

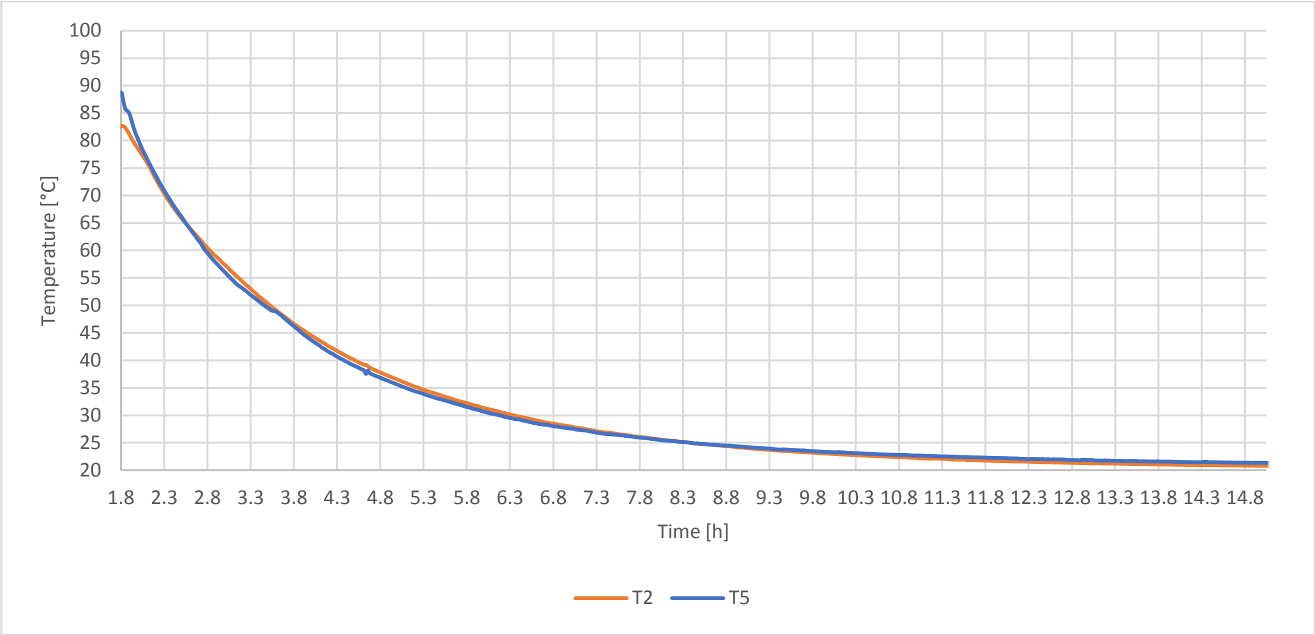

Annex 10 - Cooling – Temperature vs. time in the center of the sample – Test 2

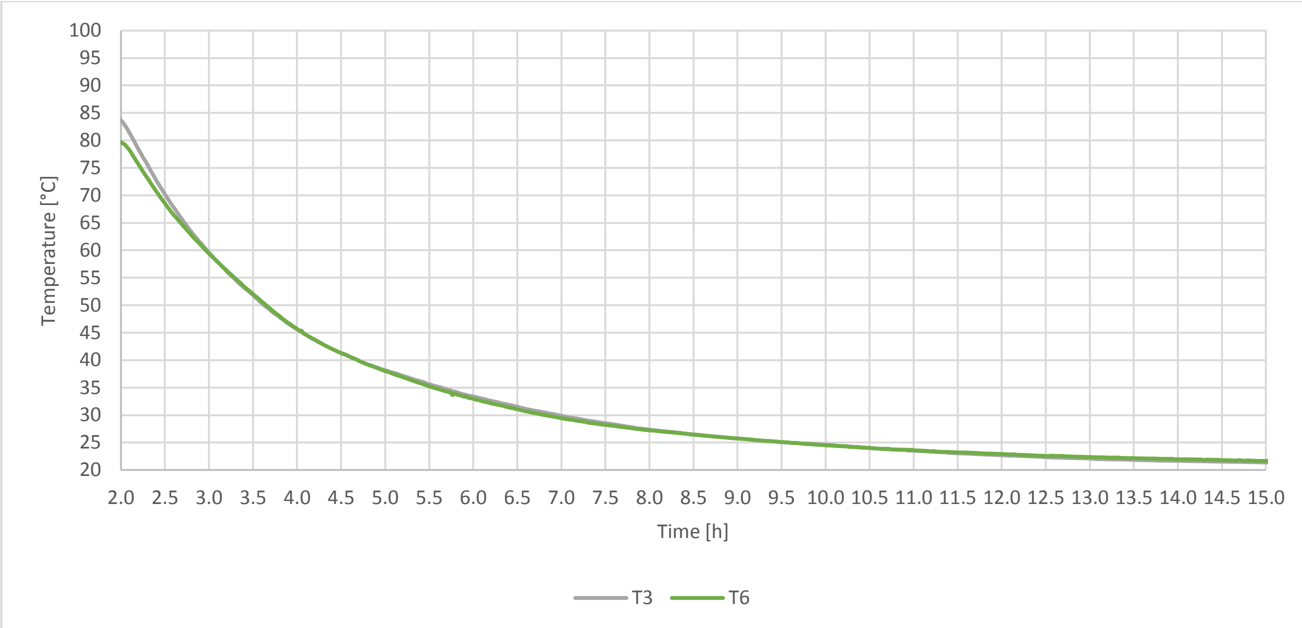

Annex 11 - Cooling – Temperature vs. time in the lower part of the sample – Test 1

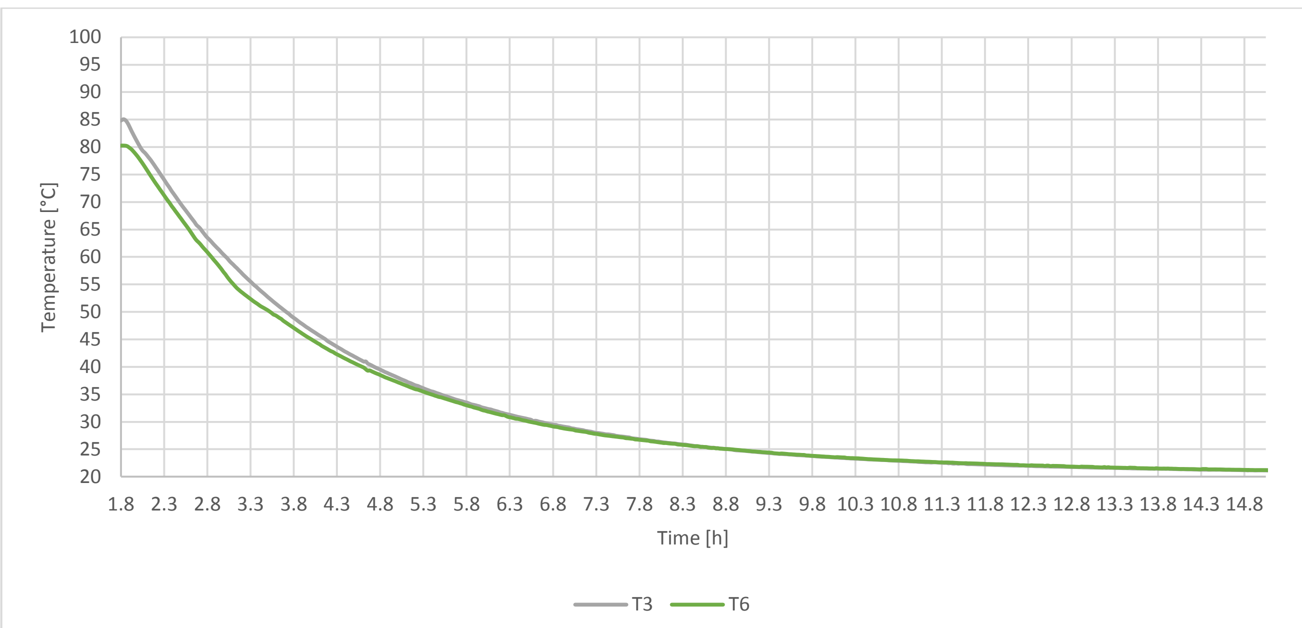

Annex 12 - Cooling – Temperature vs. time in the lower part of the sample – Test 2